Int. J. Heat Mass Transfer. Vol. 21, pp. 15–23. Pergamon Press 1978. Printed in Great Britain

GROWTH OF A VAPOUR BUBBLE IN COMBINED GRAVITATIONAL AND NON-UNIFORM TEMPERATURE FIELDS

J. G. H. JOOSTEN,* W. ZIJL and S. J. D. VAN STRALEN
Laboratory for Fluid Dynamics and Heat Transfer, Eindhoven University of Technology, Eindhoven, The Netherlands

(*Received* 4 *October* 1976)

Abstract—The growth of rotationally symmetric vapour bubbles on a horizontal plane has been studied by solving the equations of motion numerically. For this purpose, the global collocation method has been applied, cf. Zijl [1]. In this way deviations from the spherical bubble shape, which are due to gravity, are considered. Restriction is made to the initial stage of contraction of the bubble contact-radius. The numerical results following from appropriate initial temperature distributions are in qualitative agreement with previous experimental data by van Stralen *et al.* [2, 3] on water, boiling at subatmospheric pressures. Quantitative agreement is obtained by fitting only one dimensional parameter, i.e. the initial height of a superheated liquid cylinder or hemisphere. Also, experimentally observed oscillations in the equivalent bubble radius during growth are introduced numerically. A physical interpretation of this phenomenon is given by van Stralen, Zijl and De Vries [4]. The frequency of these oscillations increases with increasing pressure, i.e. with increasing vapour density. In addition, both the thickness of the thermal boundary layer around the bubble and the instantaneous locations of the isotherms in the surrounding liquid are calculated.

NOMENCLATURE

a, $(=k/\rho c)$, liquid thermal diffusivity [m^2/s];
A, area of the bubble cap [m^2];
$a_k(t)$, expansion coefficient in a series;
$b_k(t)$, expansion coefficient in a series;
c, liquid specific heat at constant pressure [J/kgK];
D, nonlinear differential operator;
$E^+(t)$, functions representing a memory effect;
$E^-(t)$, of the heat diffusion process [m/s];
F, $2N+2$ dimensional vector function;
g, gravitational acceleration [m/s^2];
H_c, height of a cylinder with superheated liquid above heating surface [m];
Ja, $\{=\rho c[\bar{T}_R(0)-T_S]/\rho_v l\}$ Jakob number for superheated liquid;
k, liquid thermal conductivity [W/mK];
K, constant number $0 < K < \infty$;
l, latent enthalpy of vaporization [J/kg];
$\mathbf{n}$, unit vector normal to bubble surface;
N, number of collocation points minus one;
p, liquid pressure [Pa];
p_v, vapour pressure [Pa];
p_R, liquid pressure at bubble boundary [Pa];
p_∞, liquid pressure at great distance from the bubble [Pa];
P_n, Legendre polynomial of order zero and degree n;
r, radial coordinate in spherical coordinate system [m];
$R(\vartheta, t)$, bubble radius in spherical coordinate system [m];
R_c, radius of a cylinder with superheated liquid above heating surface [m];
R_s, radius of hemisphere with superheated liquid above heating surface [m];
R_{eq}, $[=(3V/4\pi)^{1/3}]$ equivalent bubble radius [m];
R_1, R_2, principal radii of curvature of the bubble boundary [m];
R_0, $(=2\sigma T_S/\rho_v l(\bar{T}_R(0)-T_S))$ equilibrium bubble radius [m];
t, time elapsed since the bubble has started growth [s];
$T(r, \vartheta, t)$, liquid temperature [K];
$\bar{T}_R(t)$, mean temperature at the bubble boundary [K];
$T_\infty(\vartheta, t)$, liquid temperature at the outer side of the thermal boundary layer [K];
$\bar{T}_\infty(t)$, mean liquid temperature at the outer side of the thermal boundary layer [K];
T_S, saturation temperature at pressure p_∞ [K];
$\bar{T}_R(0)$, initial vapour temperature at the time of nucleation [K];
$\mathbf{u}$, liquid velocity vector [m/s];
$\mathbf{u}_v$, vapour velocity vector [m/s];
V, volume of the bubble [m^3];
z, distance normal to the bubble boundary [m].

Greek symbols

Γ, gamma function;
δ, thickness of the thermal boundary layer [m];
ϑ, azimuthal angle in spherical coordinate system;
θ_0, $[\bar{T}_R(0)-T_S]$ initial superheating of the vapour in the bubble [K];

* Present address: Van't Hoff Laboratory, State University of Utrecht, Utrecht, The Netherlands.

μ, ($=\cos\vartheta$) azimuthal cosine;
ν, liquid kinematic viscosity [m^2/s];
ρ, liquid density [kg/m^3];
ρ_v, vapour density [kg/m^3];
σ, surface tension coefficient at liquid vapour interface [N/m];
ϕ, liquid velocity potential [m^2/s].

Subscripts
i, number of a temperature point on a line characterized by ϑ_j;
j, number of collocation angle ϑ_j;
∞, at great distance from the bubble;
R, at the bubble boundary.

Superscripts
$\bar{\ }$, mean value;
$\dot{\ }$, differentiation with respect to time [$1/s$];
$\tilde{\ }$, approximate value.

1. INTRODUCTION

1.1. *Previous investigations*

Effect of bubbles on heat transfer. Vapour bubbles have a substantial influence on nucleate boiling heat transfer, and result in an augmentation of the corresponding convective contribution. This is the case both in saturated and in subcooled boiling, where the bubbles implode rapidly after initial growth.

The relaxation microlayer theory by van Stralen [5] expresses both bubble behaviour and bubble-induced heat transfer at the wall into convection. Recently, this model has been extended to combine the contribution to bubble growth due to the relaxation microlayer (around the lower part of the curved bubble boundary) with the contribution due to heat transmission through an evaporating microlayer (beneath the bubble), cf. [2]. The initial superheating enthalpy of both microlayers is taken from the corresponding convective thermal boundary layer at the wall, which is renewed during the waiting time between succeeding bubbles generated at the same nucleation site.

Bubble growth rates. Initial (isothermal) bubble growth is governed by liquid inertia, i.e. the bubble is blown up due to an excess pressure, which results from a superheating of the vapour. This superheating decreases gradually due to evaporation at the bubble boundary, until advanced (isobaric) bubble growth is determined by heat- (and mass-) diffusion.

The theoretical predictions are in quantitative agreement with experimental data on water boiling at various subatmospheric pressures. In this model the relative height of the relaxation microlayer is fitted to the experimental bubble departure radius [3]. Both the bubble radius and the departure time increase substantially with decreasing pressure. At pressures below 3 kPa, the superheating of the bubble boundary decreases only slightly, resulting in the occurrence of large "Rayleigh bubbles" [3]. The effect of gravity, which causes detachment, has not been incorporated into this model [2] and another disadvantage is the empirical description of the transition between the modes of initial and diffusion-controlled growth.

1.2. *Scope of the present investigations*

Bubble oscillations. It has been shown by van Stralen, Zijl and De Vries [4], using the theory of fractional derivatives [6], that both the volume and the temperature of free vapour bubbles may oscillate during growth. The nature of these oscillations originates from combined liquid inertia and transient heat conduction, which causes the changes in liquid velocity to lay behind changes in excess pressure. Similar oscillations in the bubble volume have been observed experimentally by van Stralen [7], and are also obvious from the data presented in [3]. At present, the growth of rotationally symmetric vapour bubbles in a gravitational field is investigated numerically by solving the Bernoulli equation for the pressure with the global collocation method, cf. Zijl [1].

Various initial temperature distributions in the superheated liquid above the horizontal wall are taken, since the initial field is expected to have a substantial effect on bubble growth rates. This effect is also incorporated into the semi-empirical treatment of Mikic *et al.* [8].

2. MATHEMATICAL FORMULATION

Since the density of the vapour in the bubble depends only on the hardly varying temperature, the vapour may be considered as incompressible. Consequently one has to start from the Navier–Stokes equations for an incompressible fluid to describe the flow- and temperature fields inside and outside a bubble.

In the present investigation, bubble growth on a flat horizontal superheated wall has been studied, cf. Fig. 1.

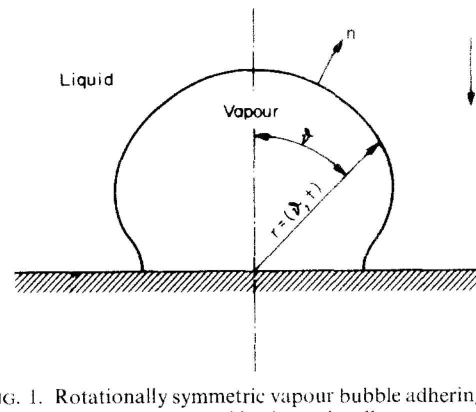

FIG. 1. Rotationally symmetric vapour bubble adhering to a superheated horizontal wall.

The heat flux at the wall has been neglected. The heating surface is assumed to be a plane of symmetry between the bubble under consideration and a "mirror bubble". Hence, the normal velocity condition $\mathbf{u}\cdot\mathbf{n} = 0$ is satisfied automatically. Furthermore, the no-slip condition does not play a role since the viscous layer, along which the liquid moves smoothly, is assumed to be thin. For the same reason no assumption needs to be made about the contact angle. In addition, it is assumed that the influence of the tangential stress condition on the bubble boundary is limited to a thin hydrodynamic boundary layer around the bubble. This assumption is based on the absence of a viscous wake behind a non-translating bubble. Under the above mentioned restrictions, potential flow theory may be applied in the liquid outside the bubble.

In order to solve the temperature field, two regions are considered: (i) a thin thermal boundary layer around the bubble, and (ii) the remaining bulk liquid. Since the thermal boundary layer has an overlap with the hydrodynamic boundary layer, the flow field in the latter can influence the heat transfer rate substantially.

To simplify the treatment, it is assumed that tangential velocities and interfacial turbulence, induced by surface-tension gradients, may be neglected. For pure systems this is a good approximation. Combination of the Bernoulli equation for the liquid pressure, the Laplace equation for the surface tension and the linearized Clapeyron equation, results in the following boundary condition, which is written in spherical coordinates, cf. [1]:

$$\frac{\mathrm{d}\phi}{\mathrm{d}t} = -\tfrac{1}{2}\left\{\left(\frac{\partial\phi}{\partial r}\right)^2 + \left(\frac{1}{R}\frac{\partial\phi}{\partial\vartheta}\right)^2\right\} - \frac{\rho_v l}{\rho T_S}(T_R - T_S) - gR\cos\vartheta - \frac{\sigma}{\rho}\frac{1}{R}\,\frac{1+2\left(\dfrac{1}{R}\dfrac{\partial R}{\partial\vartheta}\right)^2 - \dfrac{1}{R}\dfrac{\partial^2 R}{\partial\vartheta^2}}{\left\{1+\left(\dfrac{1}{R}\dfrac{\partial R}{\partial\vartheta}\right)^2\right\}^{3/2}} + \frac{1-\dfrac{1}{R}\dfrac{\partial R}{\partial\vartheta}\dfrac{\cos\vartheta}{\sin\vartheta}}{\left\{1+\left(\dfrac{1}{R}\dfrac{\partial R}{\partial\vartheta}\right)^2\right\}^{1/2}} + \frac{\partial\phi}{\partial r}\frac{\mathrm{d}R}{\mathrm{d}t}, \tag{1}$$

on $r = R(\vartheta, t)$.

Combination of the terms $\mathrm{d}\phi/\mathrm{d}t - (\partial\phi/\partial r)(\mathrm{d}R/\mathrm{d}t) = \partial\phi/\partial t$ represents the unsteady inertia part of the Bernoulli equation; the first term on the RHS represents the convective inertia part. The second term represents the pressure difference, calculated with the Clapeyron equation. The third term describes the effect of gravity and the fourth term considers the compound bubble radius. In the examples presented here, the latter term was always small with respect to other terms. The heat requirement for evaporation or condensation at the bubble boundary is given by the flux balance:

$$k\nabla T\cdot\mathbf{n} = \rho_v l(\nabla\phi - \mathbf{u}_v)\cdot\mathbf{n}, \tag{2}$$

on $r = R(\vartheta, T)$.

The condition that the flow velocity equals the displacement rate of the bubble boundary is expressed by:

$$\frac{\mathrm{d}R}{\mathrm{d}t} = \frac{\partial\phi}{\partial r} - \frac{1}{R^2}\frac{\partial R}{\partial\vartheta}\frac{\partial\phi}{\partial\vartheta}. \tag{3}$$

The boundary conditions (1)–(3), combined with the Laplace equation for the velocity potential and the heat diffusion equation for the temperature, represent a well-posed partial differential problem if initial conditions are prescribed.

3. THE NUMERICAL METHOD

3.1. *The flow field*

The solution of the potential equation with zero velocity for $r \to \infty$, symmetric with respect to the plane $\vartheta = \frac{1}{2}\pi$ and non-singular at $\vartheta = 0$ is:

$$\phi(r, \vartheta, t) = \sum_{k=0}^{\infty} a_k(t)\frac{1}{r^{2k+1}}P_{2k}(\cos\vartheta). \tag{4}$$

Also, the radius of the bubble boundary is expanded in even Legendre polynomials:

$$R(\vartheta, t) = \sum_{k=0}^{\infty} b_k(t)P_{2k}(\cos\vartheta). \tag{5}$$

The expansion coefficients $a_k(t)$, $b_k(t)$ can be determined by matching the general expressions (4) and (5) to the boundary conditions (1) and (3). This has to be done numerically and for reasons of computational efficiency, the collocation method has been used, cf. Finlayson [9]. In this method, the series (4) and (5) are truncated after $N+1$ terms and the bubble boundary is discritized into a number of $N+1$ so-called "collocation points". The boundary conditions (1) and (3) are applied on these points only. This procedure results in a set of coupled, non-linear ordinary differential equations for the bubble radius on the collocation angles $\{\vartheta_i\}_{i=0}^{N}$ and for the velocity potential on the collocation points $\{\tilde{R}(\vartheta_{i,k}), \vartheta_i\}_{i=0}^{N}$.

$$\frac{\mathrm{d}}{\mathrm{d}t}\begin{pmatrix}\tilde{R}_i\\ \tilde{\phi}_i\end{pmatrix} = F[\{\tilde{R}_j, \tilde{\phi}_j\}_{j=0}^{N}], \quad i = O(1)N, \tag{6}$$

where:

$$\tilde{R}_i(t) = \tilde{R}(\vartheta_i, t) = \sum_{k=0}^{N}[P_{2k}(\cos\vartheta_i)]\tilde{b}_k(t), \tag{7}$$

$$\phi_i(t) = \tilde{\phi}(\tilde{R}_i(t), \vartheta_i, t) = \sum_{k=0}^{N}\left[\left(\frac{1}{R_i(t)}\right)^{2k+1}P_{2k}(\cos\vartheta_i)\right]\tilde{a}_k(t). \tag{8}$$

Numerically spoken, F is a subroutine in which at every timestep the matrix-equations (7) and (8) have to be solved. Since these matrices are not sparse, the number of collocation points may not be too high and special attention must be given to the scaling. Let boundary conditions (1) and (3) be represented by:

$$\left[D\begin{pmatrix}R(\mu, t)\\ \phi(r, \mu, t)\end{pmatrix}\right]_{r=R(\mu,t)} = 0. \tag{9}$$

From interpolation theory it follows, that for the approximate solutions $\tilde{R}(\mu, t)$ and $\tilde{\phi}(r, \mu, t)$ the following inequality holds if the collocation cosines are taken as the zeros of a Chebyshev polynomial, cf. Fox and Parker [10]:

$$\left[D\begin{pmatrix}\tilde{R}(\mu, t)\\ \tilde{\phi}(r, \mu, t)\end{pmatrix}\right]_{r=\tilde{R}(\mu,t)} < \frac{K}{2^N(N+1)!}. \tag{10}$$

If the zeros of a Legendre polynomial are used, the RHS of (19) has to be multiplied by $(N+1)^{1/2}$. For stably growing vapour bubbles, small variations in the initial and boundary conditions will result in small variations of the flow field. Hence, it follows from (10) that $\tilde{R}_i$, $\tilde{\phi}_i$ converge to the exact solution for $N \to \infty$.

3.2. *The thermal boundary layer*

For a thin thermal boundary layer the heat diffusion equation may be simplified to:

$$\frac{\partial T}{\partial t} = a\frac{\partial^2 T}{\partial z^2}. \quad (11)$$

Combination of equation (11) with heat flux boundary condition (2) results in, cf. [4]:

$$T_R(\vartheta, t) = T_\infty(\vartheta) - \frac{\rho_v l}{\rho c}\frac{1}{a^{1/2}}\frac{\mathrm{d}^{-1/2}}{\mathrm{d}t^{-1/2}}(\nabla\phi - \mathbf{u}_v)_{r=R(\vartheta,t)}\cdot\mathbf{n}. \quad (12)$$

In (12) the fractional notation is introduced, cf. [4, 6]. In every collocation point equation (12) has to be solved simultaneously with equation (6) for the bubble radius and the velocity potential. In principle also the flow field $\mathbf{u}_v$ in the vapour has to be solved, however, the vapour flow and temperature fluctuate rapidly with respect to changes in liquid flow and temperature. This convective phenomenon is due to the small density ratio $\rho_v/\rho \ll 1$, which causes that the vapour accelerates in a timescale small in comparison with the timescale in which the liquid is accelerated.

Consequently, on the timescale in which bubble growth takes place only a mean temperature $\overline{T}_R(t)$ is observed. Furthermore, since $\rho_v/\rho \ll 1$, a small volume of liquid, evaporated at the bubble boundary, is transformed into a big volume of vapour. Consequently the bubble grows because it is blown up and not because liquid is removed by evaporation at the bubble cap. From the above discussion it is concluded that distortions in the bubble shape can only be explained by gravity and not by the different rates of evaporation or condensation at the vapour–liquid interface.

Now in equation (12) the mean vapour temperature $\overline{T}_R(t)$ has to be inserted. By taking the mean value of equation (12) it is found that:

$$\overline{T}_R(t) = \overline{T}_\infty - \frac{\rho_v l}{\rho c}\frac{1}{a^{1/2}}\frac{\mathrm{d}^{-1/2}}{\mathrm{d}t^{-1/2}}\overline{\nabla\phi\cdot\mathbf{n}}. \quad (13)$$

where

$$A(t) = 2\pi\int_{\vartheta=0}^{1/2\pi} R^2(\vartheta, t)\sin\vartheta\,\mathrm{d}\vartheta, \quad (14)$$

$$\overline{\mathbf{u}_v\cdot\mathbf{n}} = \frac{2\pi}{A}\int_{\vartheta=0}^{1/2\pi}(\mathbf{u}_v\cdot\mathbf{n})_{r=R}R^2\sin\vartheta\,\mathrm{d}\vartheta = 0, \quad (15)$$

$$\overline{\nabla\phi\cdot\mathbf{n}} = \frac{2\pi}{A}\int_{\vartheta=0}^{1/2\pi}(\nabla\phi\cdot\mathbf{n})_{r=R}R^2\sin\vartheta\,\mathrm{d}\vartheta, \quad (16)$$

$$\overline{T}_\infty = \frac{2\pi}{A}\int_{\vartheta=0}^{1/2\pi}T_\infty(\vartheta)R^2\sin\vartheta\,\mathrm{d}\vartheta. \quad (17)$$

Equation (15) states that there is no net in- and outflow of vapour through the bubble cap.

In order to be able to solve equation (13) numerically, equation (13) is transformed by use of the Grünwald definition of semi derivatives, cf. [4, 6]:

$$\frac{\mathrm{d}}{\mathrm{d}t}\left(\frac{\overline{T}_R - \overline{T}_\infty}{\overline{T}_R(0) - T_S}\right)^2 = \frac{2}{a}\frac{1}{Ja^2}(\overline{\nabla\phi\cdot\mathbf{n}} + E^+)(\overline{\nabla\phi\cdot\mathbf{n}} - E^-), \quad (18)$$

$$E^+(t) = \lim_{N\to\infty}\frac{1}{\pi^{1/2}}\sum_{j=1}^{N-1}\frac{\Gamma(j+\frac{1}{2})}{\Gamma(j+1)}\overline{\nabla\phi\cdot\mathbf{n}}\left(t - \frac{jt}{N}\right), \quad (19)$$

$$E^-(t) = \lim_{N\to\infty}\frac{1}{2\pi^{1/2}}\sum_{j=1}^{N-1}\frac{\Gamma(j-\frac{1}{2})}{\Gamma(j+1)}\overline{\nabla\phi\cdot\mathbf{n}}\left(t - \frac{jt}{N}\right). \quad (20)$$

The functions (19) and (20) are evaluated at time $t - it/N$ and they represent a memory effect. Since the effect of gravity on the bubble shape and not the coupling between the hydrodynamic and thermal equations is the aim of this study, the set (18)–(20) is roughly approximated by putting $E^+ = E^- = 0$ and when $\overline{\nabla\phi\cdot\mathbf{n}}$ changes sign, $\overline{T}_R$ is made discontinuously equal to $\overline{T}_\infty$. In this way oscillations are introduced artificially. These oscillations have a physical meaning as discussed below.

When other bubbles suddenly start growing in the neighbourhood of the bubble under consideration, the bubble reacts on such a pressure step in a damped oscillatory way, cf. [4]. Consequently, the oscillations introduced here, represent a surrounding with growing bubbles; the amplitude is artificial but the frequency equals the eigenfrequency of the bubble. Note also the agreement with the experimental values presented in Figs. 5 and 7.

3.3. *The bulk liquid*

In this region, heat transport is assumed to take place by convection only. On $t = 0$, a mesh with temperatures $T_{ij} = T(r_i, \vartheta_j, 0)$ is prescribed. Since these temperatures are fixed to moving fluid elements, the coordinates $[r_i(t), \vartheta_j(t)]$ of temperature T_{ij} can be calculated from the flow velocity $\mathbf{u}(r_i, \vartheta_j, t) = \nabla\phi$. In order to simplify the calculations, the flow has been assumed radial so that ϑ_j is independent of time. The thermal boundary-layer thickness $\delta(\vartheta_j, t)$ is approximated.

Addition of $\delta(\vartheta_j, t)$ to $R(\vartheta_j, t)$ gives the position of $T_\infty(\vartheta_j, t)$; the value of it is determined by linear interpolation.

4. ROTATIONALLY SYMMETRIC BUBBLE GROWTH

4.1. *Effect of initial temperature distribution*

In order to avoid the difficult problem of calculating or measuring the real initial temperature distribution, the solution of $\nabla^2 T = 0$ in a cylinder or hemisphere is used, cf. Fig. 2. Figure 3 compares the results for a hemisphere and a cylinder. Figure 4 shows that an increase in the initial superheated cylinder height H_c results in an increase in the growth rate.

4.2. *Comparisons with experimental data*

Figures 5 and 6 show the equivalent bubble radius and the bubble shape, respectively.

The changes in bubble shape are due to gravity only, since thermal effects may be neglected by using a mean temperature. Also, gradients in surface tension have been neglected. A comparison with experimental data, cf. van Stralen *et al.* [2] is made. Figures 5 and 6

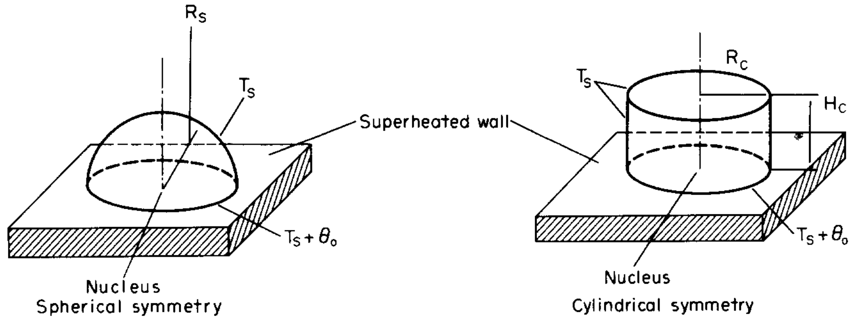

FIG. 2. Liquid hemisphere and cylinder with boundary conditions for the temperature. The solution of the Laplace equation $\nabla^2 T = 0$ is used as initial temperature distribution.

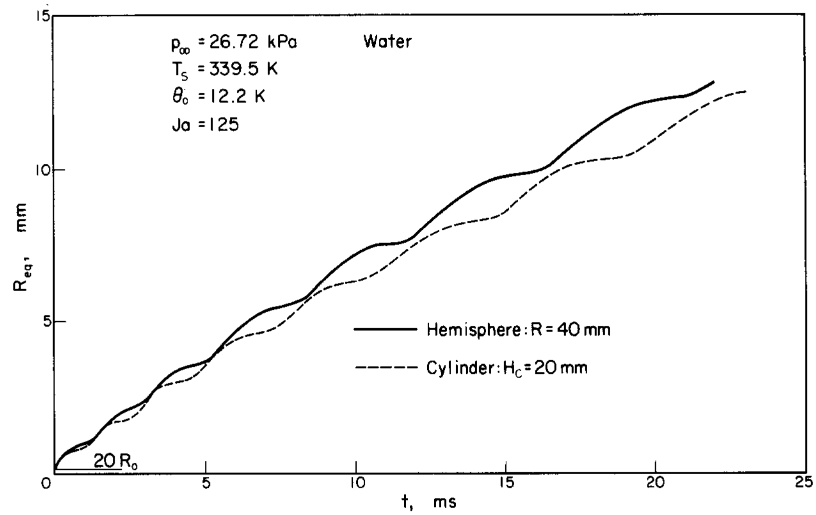

FIG. 3. *Water boiling at* 26.72 kPa. Effect of a spherically symmetric (——) and a cylindrically symmetric (– – –) temperature field, respectively, on bubble growth.

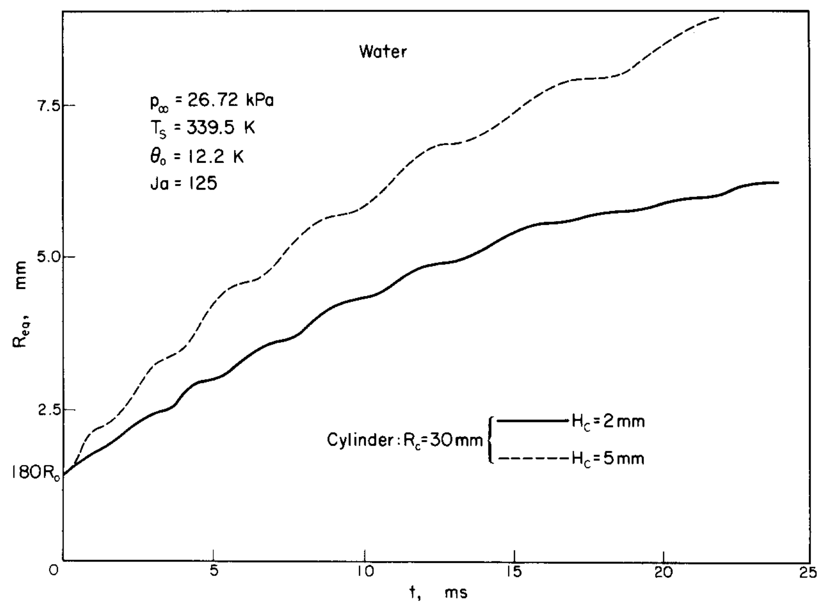

FIG. 4. *Water boiling at* 26.72 kPa. Bubble growth curve for various cylindrically symmetric temperature fields.

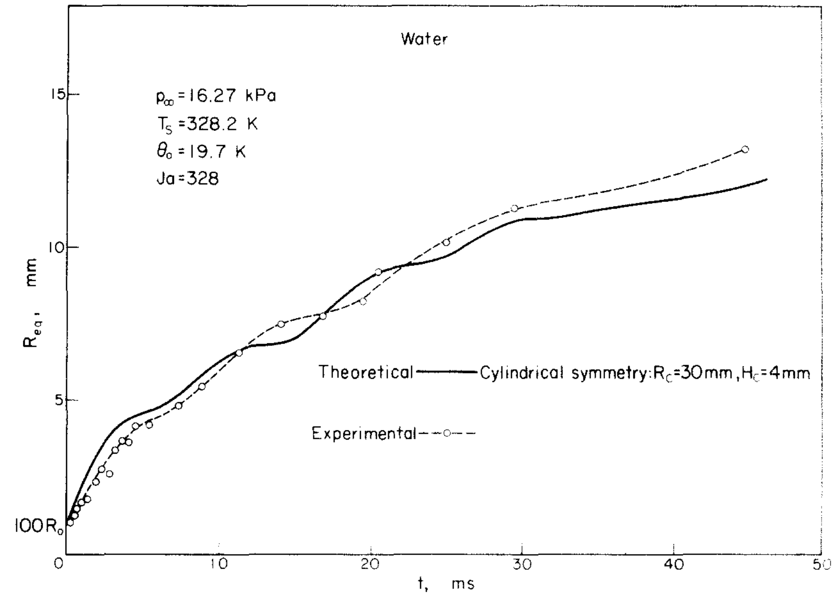

FIG. 5. *Water boiling at* 16.27 kPa. Comparisons between experimental (--o o--) and numerical (——) equivalent bubble growth curve.

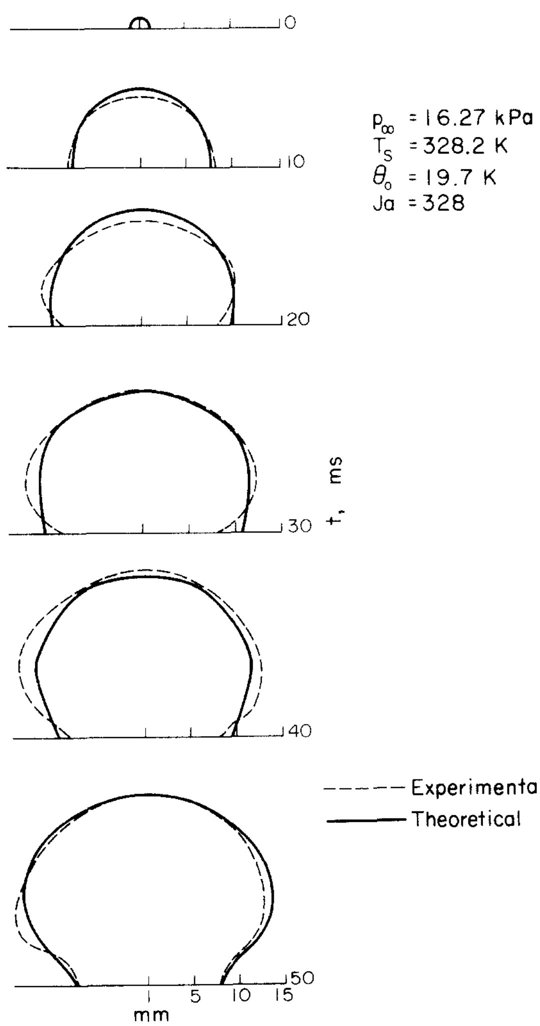

FIG. 6. *Water boiling at* 16.27 kPa. Profile of the vapour bubble shown in Fig. 6 at various instants. The bubble contraction due to gravity is compared with experimental data.

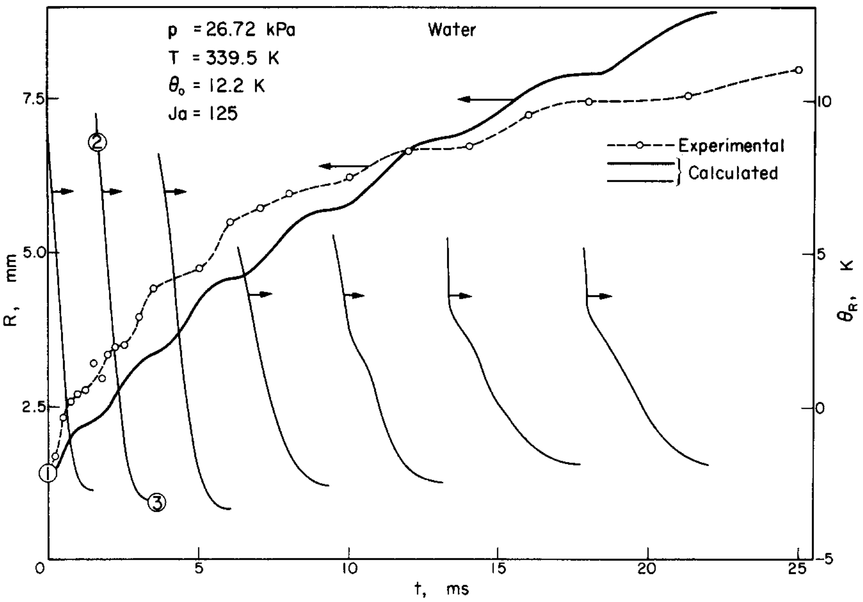

FIG. 7. *Water boiling at* 26.72 kPa, cf. Fig. 4. Comparison between experimental (--o--o--) and numerical (——) bubble growth curve. $H_c = 5$ mm; $R_c = 30$ mm.

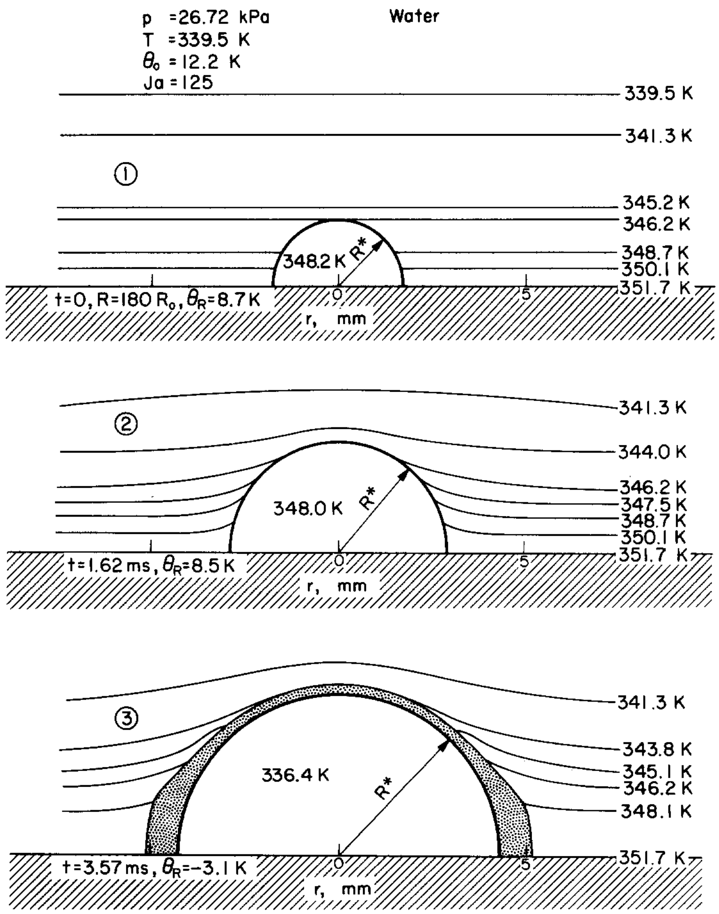

FIG. 8. *Water boiling at* 26.72 kPa. Computed isotherms around the bubble of Fig. 8. The edge of the thermal boundary layer has been dotted.

correspond with Fig. 5, cf. [2], Fig. 7 corresponds with Fig. 3, cf. [2]. It may be noticed, that the original value of the Jakob number has been changed here by taking the hydrostatic pressure in account. In Fig. 8 the calculated isotherms are shown around the bubble depicted in Fig. 7.

5. CONCLUSION

The gross features of the computed data can be fitted to the measured data by choosing the initial temperature field suitably. Only when the actual temperature distribution is measured experimentally and when the thermal diffusion equation is solved more accurately, an estimation can be made of the effect of a thin evaporating liquid microlayer beneath a growing bubble.

REFERENCES

1. W. Zijl, Global collocation approximations of the flow and temperature fields around a gas and a vapour bubble. *Int. J. Heat Mass Transfer* **20**, 487–498 (1977).
2. S. J. D. van Stralen, M. S. Sohal, R. Cole and W. M. Sluyter, Bubble growth rates in pure and binary systems: combined effect of relaxation and evaporation microlayer, *Int. J. Heat Mass Transfer* **18**, 453–467 (1975).
3. S. J. D. van Stralen, R. Cole, W. M. Sluyter and M. S. Sohal, Bubble growth rates in nucleate boiling of water at subatmospheric pressures, *Int. J. Heat Mass Transfer* **18**, 655–669 (1975).
4. S. J. D. van Stralen, W. Zijl and D. A. De Vries, The behaviour of vapour bubbles at subatmospheric pressures, *Chem. Engng Sci.* To be published.
5. S. J. D. van Stralen, The mechanism of nucleate boiling in pure liquids and in binary mixtures, Parts I–IV, *Int. J. Heat Mass Transfer* **9**, 995–1020, 1021–1046 (1966); **10**, 1469–1484, 1485–1498 (1967).
6. K. B. Oldham and J. Spanier, *The Fractional Calculus*. Academic Press, New York (1974).
7. S. J. D. van Stralen, The growth rate of vapour bubbles in superheated pure liquids and binary mixtures, Parts I–II, *Int. J. Heat Mass Transfer* **11**, 1467–1490, 1491–1512 (1968).
8. B. B. Mikic, W. M. Rohsenow and P. Griffith, On bubble growth rates, *Int. J. Heat Mass Transfer* **13**, 657–666 (1970).
9. B. A. Finlayson, The method of weighted residuals and variational principles, in *Mathematics in Science and Engineering*, Vol. 87. Academic Press, New York (1972).
10. L. Fox and I. B. Parker, *Chebyshev Polynomials in Numerical Analysis*. Oxford University Press, London (1968).

CROISSANCE D'UNE BULLE DE VAPEUR DANS LES CHAMPS COUPLES DE GRAVITATION ET DE TEMPERATURE NON UNIFORME

Résumé—La croissance des bulles de vapeur symétriques rotationnellement, sur une plaque horizontale, a été étudiée en résolvant numériquement les équations du mouvement. On a appliqué pour cela la méthode globale de collocation, cf. Zijl [1]. On considère les déviations à partir de la forme sphérique, lesquelles sont dues à la gravité. Une restriction est faite pour le stade initial de contraction du rayon de contact de la bulle.

Les résultats numériques pour des distributions initiales de température appropriées sont en bon accord qualitatif avec des expériences antérieures de Van Stralen *et al.* [2, 3] sur l'eau, bouillant à des pressions subatmosphériques. Un accord quantitatif est obtenu en ajustant seulement un paramètre adimensionnel, la hauteur initiale du cylindre ou de l'hémisphère de liquide surchauffé. On introduit numériquement les oscillations observées expérimentalement dans le rayon équivalent de bulle pendant la croissance. Une interprétation physique de ce phénomène est donnée par Van Stralen, Zijl et de Vries [4].

La fréquence de ces oscillations croît avec l'augmentation de la pression, donc de la densité de la vapeur. On calcule en outre l'épaisseur de la couche limite thermique autour de la bulle et les positions instantanées des isothermes dans le liquide environnant.

DAS WACHSTUM VON DAMPFBLASEN IN KOMBINIERTEN GRAVITATIONS- UND UNGLEICHFÖRMIGEN TEMPERATURFELDERN

Zusammenfassung—Durch numerisches Lösen der Bewegungsgleichungen wurde das Wachstum rotationssymmetrischer Dampfblasen auf einer horizontalen, ebenen Fläche untersucht. Dabei wurde die globale Kollokationsmethode nach Zijl [1] angewandt. Schwerkraftbedingte Abweichungen von der sphärischen Blasenform werden hierbei berücksichtigt. Einschränkungen werden für das anfängliche Stadium mit Kontraktion des Blasen-Kontaktradius geltend gemacht. Die aus geeigneten Anfangstemperaturfeldern ermittelten numerischen Ergebnisse stimmen qualitativ mit früheren Meßergebnissen von van Stralen u.a. [2, 3] für siedendes Wasser bei Unterdruck überein. Eine quantitative Übereinstimmung wird durch Anpassen eines einzigen dimensionslosen Parameters, nämlich der Anfangshöhe eines Zylinders oder einer Halbkugel aus überhitzter Flüssigkeit, erzielt. Die experimentell beobachteten Oszillationen des äquivalenten Blasenradius während des Wachstums werden ebenfalls numerisch eingeführt. Eine physikalische Erklärung dieses Phänomens wird von van Stralen, Zijl und de Vries [4] gegeben. Die Frequenz dieser Oszillationen nimmt mit steigendem Druck, d.h. mit steigender Dampfdichte zu. Zusätzlich werden sowohl die Dicke der thermischen Grenzschicht um die Blase wie die augenblicklichen Lagen der Isothermen in der umgebenden Flüssigkeit berechnet.

РОСТ ПУЗЫРЯ ПАРА В ГРАВИТАЦИОННОМ И НЕОДНОРОДНОМ ТЕМПЕРАТУРНОМ ПОЛЕ

Аннотация — В работе исследуется рост осесимметричных пузырей пара на горизонтальной пластине на основе численного решения уравнений движения с помощью глобального коллакационного метода [1]. Рассмотрены случаи отклонения формы пузыря от сферической за счет силы тяжести и ограничения на начальной стадии уменьшения контактного радиуса пузыря. Результаты расчетов соответствующих распределений начальной температуры качественно совпадают с экспериментальными данными Ван Штралена и др. [2, 3] по кипению воды при давлении, ниже атмосферного. Количественное согласие достигнуто путем подбора только одного размерного параметра — начальной высоты цилиндрического или полусферического объема перегретой воды. В численном виде представлены пульсации эквивалентного радиуса пузыря во время роста. Физическое толкование этого явления приводится в работах Ван Штралена, Зийля и Де Вриза [4]. Частота пульсаций возрастает с увеличением давления, т. е. с увеличением плотности пара. Кроме того, рассчитаны толщина теплового пограничного слоя вокруг пузыря и мгновенное расположение изотерм в окружающей жидкости.